Stellar activity, rotation, ages

Antonino Francesco Lanza

INAF-Osservatorio Astrofisico di Catania, Italy

Email: antonino.lanza@inaf.it

PLATO Ground Observing Program Workshop - 17-19 October 2022, Geneva, Switzerland

The complex interplay between rotation, convection, and magnetism in late-type stars

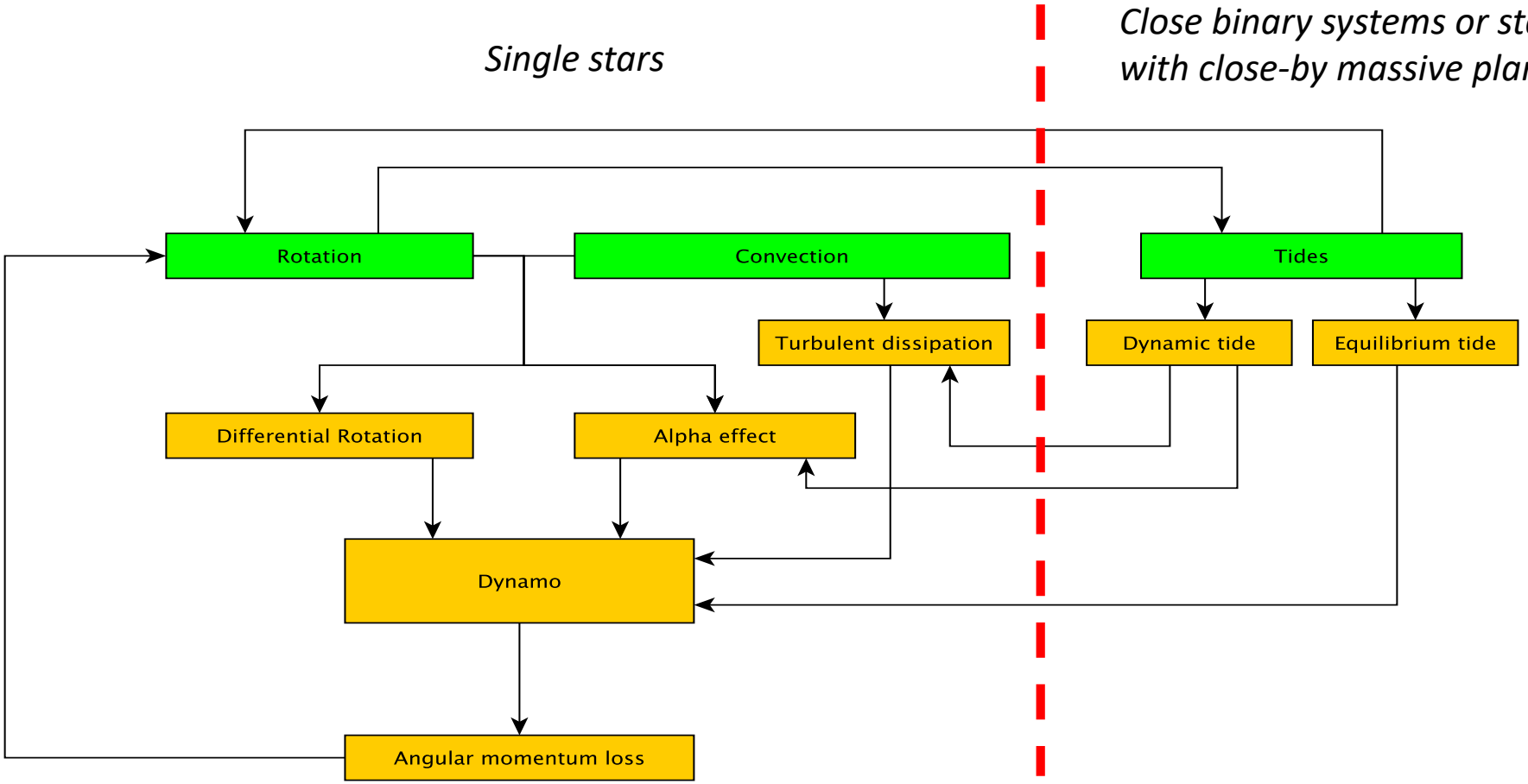

Requirements for activity indexes from the Interface Document between Stellar Science (WP12) and GOP (WP14)

(T. Morel et al. 2022; PLATO-ULG-PSM-IRD-0003)

Table 1: Summary of requirements. The technical information still TBD or TBC is highlighted in red.

Data type	Requirements from	Priority status for each sample	Data requested	Quality requested	Metadata requested
Chromospheric activity index from Ca II H & K (both $R'_{\rm HK}$ and S index)	WP122 + WP123	WP122: P1-P2 (B), P4-P5 (C) WP123: P1-P2-P4-P5 (A)	Activity index + range of variations if repeated observations[a]	Based on spectra with $R \geq$ 2500-3000 + SNR@390 $\geq$ 10	B–V, SNR@390, stellar mass, [Fe/H], luminosity class
Chromospheric activity index from Hα	WP123	P1-P2-P4-P5 (B)	Activity index + range of variations if repeated observations[a]	Based on spectra with $R \geq$ 2500-3000 + SNR@650 $\geq$ 10	B–V, SNR@650
(either preparatory or FU)				<SNR> $\geq$ 100	λ-dependent error of the data + others TBD
		P4 (B)	Near-IR spectra (TBC)[a,b]	TBD	TBD
Interferometry	WP122	P2 (B)	Calibrated OI data (oifits format)	$R \sim$ 200, SNR$_{V^2}$ > 10, 2 sets, 600-900 nm + H band (K band in option)	Instrument mode, reference stars used (+ diameter)

[a]: Securing multiple observations is not a requirement.
[b]: Whether optical and/or near-IR spectra are needed is under investigation by M-dwarf WG led by Ulrike Heiter in WP122300.

The Hα index is less useful in activity-age relationships because this line is photoionization-dominated in solar-like stars, while the Ca II H&K resonance lines are collision-dominated (i.e., directly linked to the electron temperature in their formation region), thus more sensitive to changes in magnetic heating (e.g., Linsky & Avrett 1970; Vernazza et al. 1981; Linsky 2019). Moreover, the Hα index can be affected by a varying proportion of chromospheric faculae and filaments in stars (Meunier & Delfosse 2009; Gomes da Silva et al. 2014; Meunier et al. 2022). For a proposed improved Hα index, see Gomes da Silva et al. (2022). For other activity indexes, potentially useful for M-type stars, see, Gomes da Silva (2011).

Gyrochronology

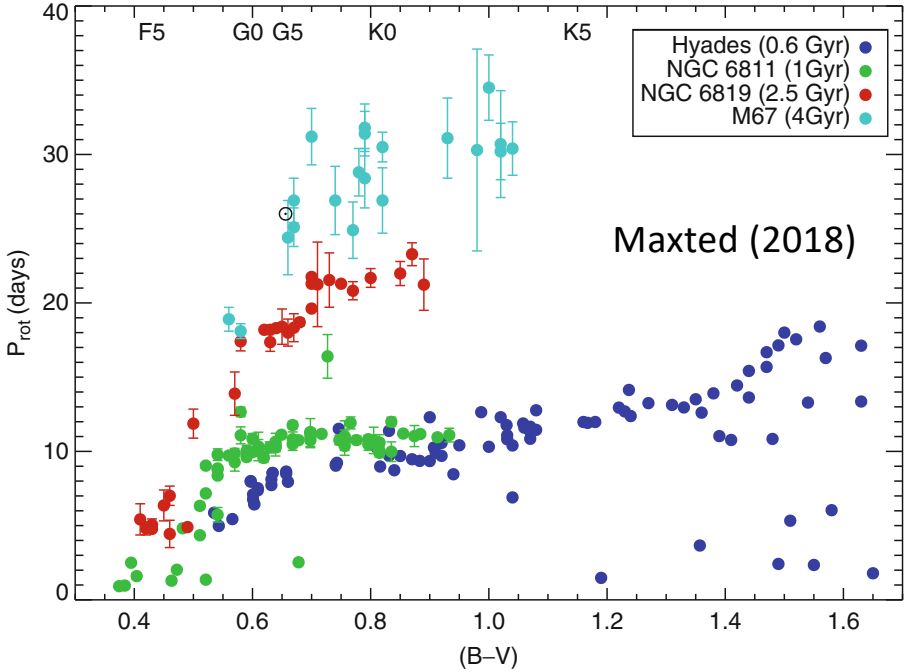

Fig. 3 Rotation periods of stars in selected open clusters and the Sun (⊙) as a function of (B−V) photometric color (Barnes et al. 2016b; Meibom et al. 2011, 2015; Radick et al. 1987, 1995)

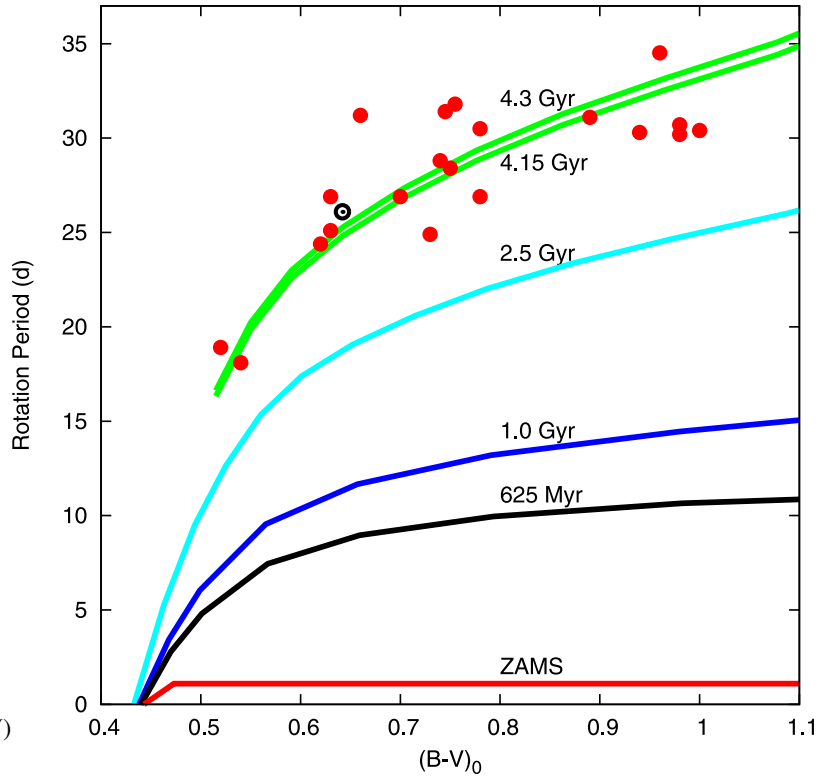

Barnes et al. (2016): rotational isochrones, the Sun, and M67 observations.

Limitations of gyrochronology: initial conditions and period measurement

a) The sensitivity of the rotation period to the initial conditions set during the PMS phase lasts for 0.5-0.8 Gyr for FGK-type stars and even longer in M-type stars;

b) Stars have surface differential rotation that limits the precision of the measurement of their rotation period (in the Sun the range is about 15%, based on chromospheric data; e.g., Donahue et al. 1996);

c) Stars have active regions with finite lifetimes; this limits or makes impossible the measurement of the rotation periods, especially at low (Sun-like) activity levels;

d) Limitation c) is especially important for stars with the age of the Sun or older; e.g., Reinhold et al. (2020) found a period measurement in only 14.5% of their *Kepler* sample of Sun-like stars analysed by McQuillan et al. (2014);

e) Methods based on the power spectrum inflection point (GPS method) gives an accuracy of ≈ 20% (Shapiro et al. 2020; Reinhold et al 2022);

The basic gyrochronology limitation: $\Delta \text{age} / \text{age} \simeq 2\,(\Delta P_{ROT} / P_{ROT})$

Further gyrochronology limitations: I. Weakened magnetic braking for old stars

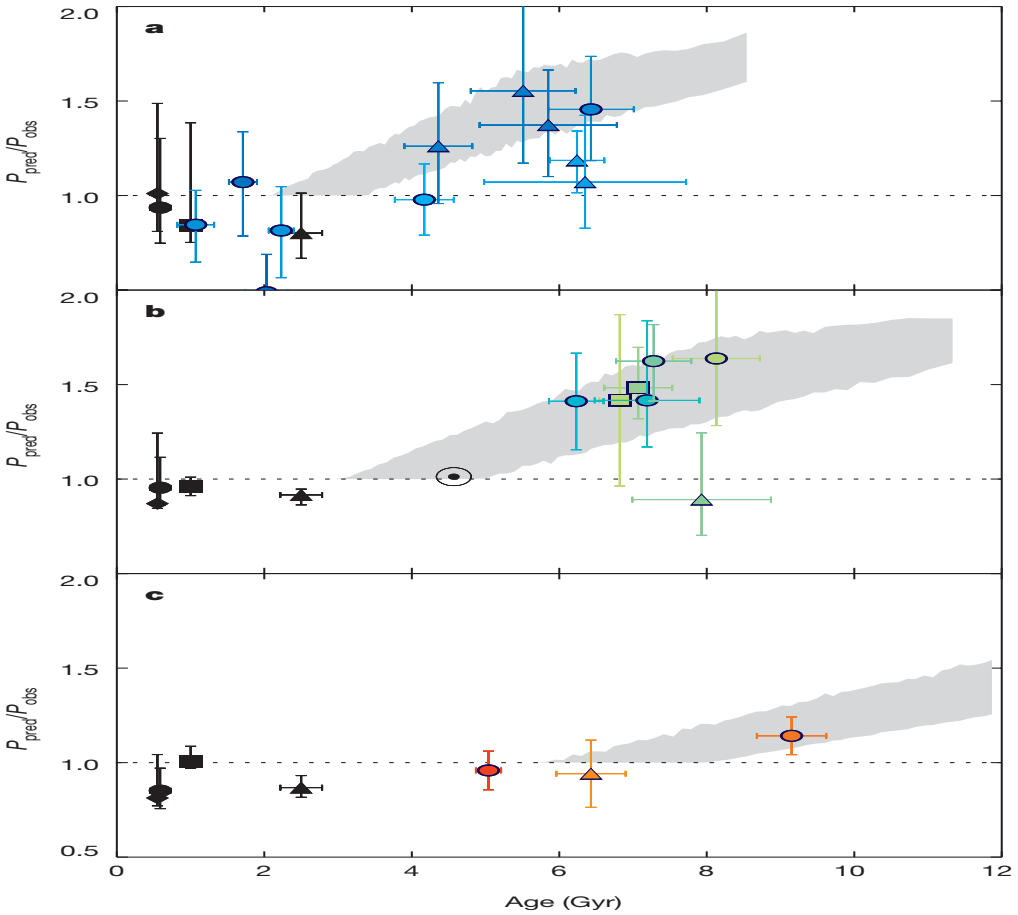

Ratio between predicted and measured rotation period in stars with asteroseismic ages in different ranges of effective temperature **a:** 5900-6200; **b:** 5600-5900; **c:** 5100-5400 K. The predicted periods come from the gyrochronological model by van Saders & Pinsonneault (2013) [Figure after van Saders et al. 2016].

Stars older than the Sun appear to experience a reduced magnetic braking. More recent works confirm this result (e.g., Hall et al. 2021 and reference therein).

Further gyrochronology limitations: II. Stalled rotation in low-mass stars

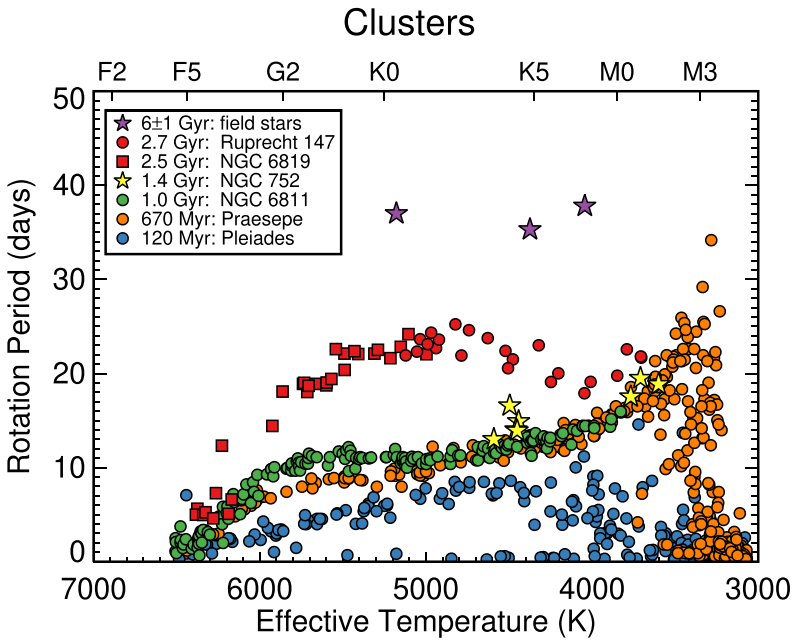

(Curtis et al. 2019)

Rotation does not appear to evolve in low-mass stars with an effective temperature between roughly 5000 and 4000 K between the age of Praesepe (0.67 Gyr) and that of NGC 6811 (1 Gyr).

The duration of the stalled rotation phase seems to be a function of the stellar mass, but we need more data for a detailed description of the phenomenon (e.g., Agueros et al. 2018; Curtis et al. 2019; Douglas et al 2019).

Stalled rotational evolution could be related to the angular momentum exchange between the radiative interior and the convective envelope in late-type stars (Spada & Lanzafame 2020).

Chromospheric activity – age relationship

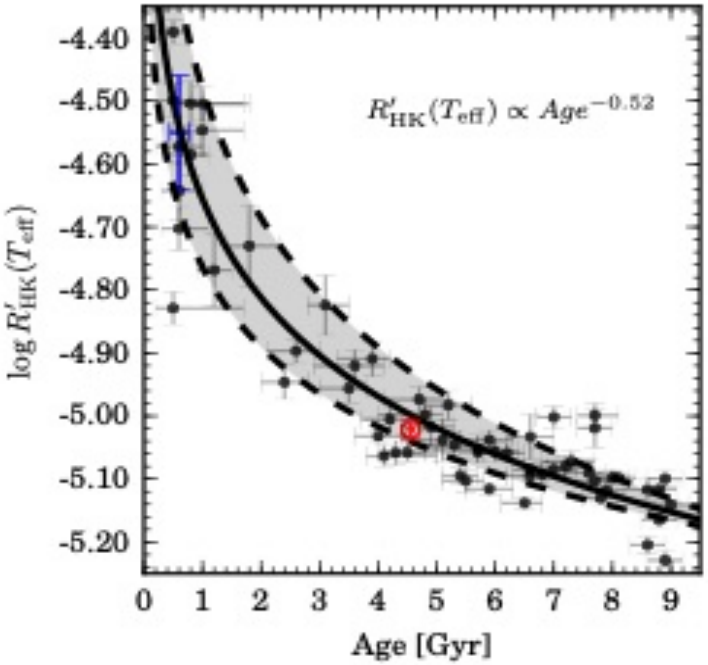

(after Lorenzo Oliveira et al. 2018 for solar twins; see also Zhang et al. 2019 for relationships based on LAMOST data for a wider range of effective temperatures)

- It appears to hold also for stars older than the Sun with the chromospheric activity indicator R'_{HK} continuing to decline up to at least 6-7 Gyr;
- *The relationship depends on the star mass* and has a maximum precision of 20-25%;
- It requires to *correct R'_{HK} for the effect of metallicity (e.g. Rocha-Pinto & Maciel 1998)*, otherwise the precision is badly reduced to 60-90%;
- It requires to properly sample the rotational cycle (usually done to apply GP models of stellar activity in RV monitoring) *and* the activity cycle (it may require monitoring on timescales of decades);

For more details, see the presentation by Joao Gomes da Silva at the HOW2 Workshop.

Effect of activity variability in age determination

- Precise activity measurements that cover the full cycles
  - **Example:**
  - Chromospheric age of Alf Cen B at cycle maximum: 5.4 +/- 0.6 Gyr (MH08)
  - Chromospheric age of Alf Cen B at cycle minimum: 9.9 +/- 1.1 Gyr (MH08)

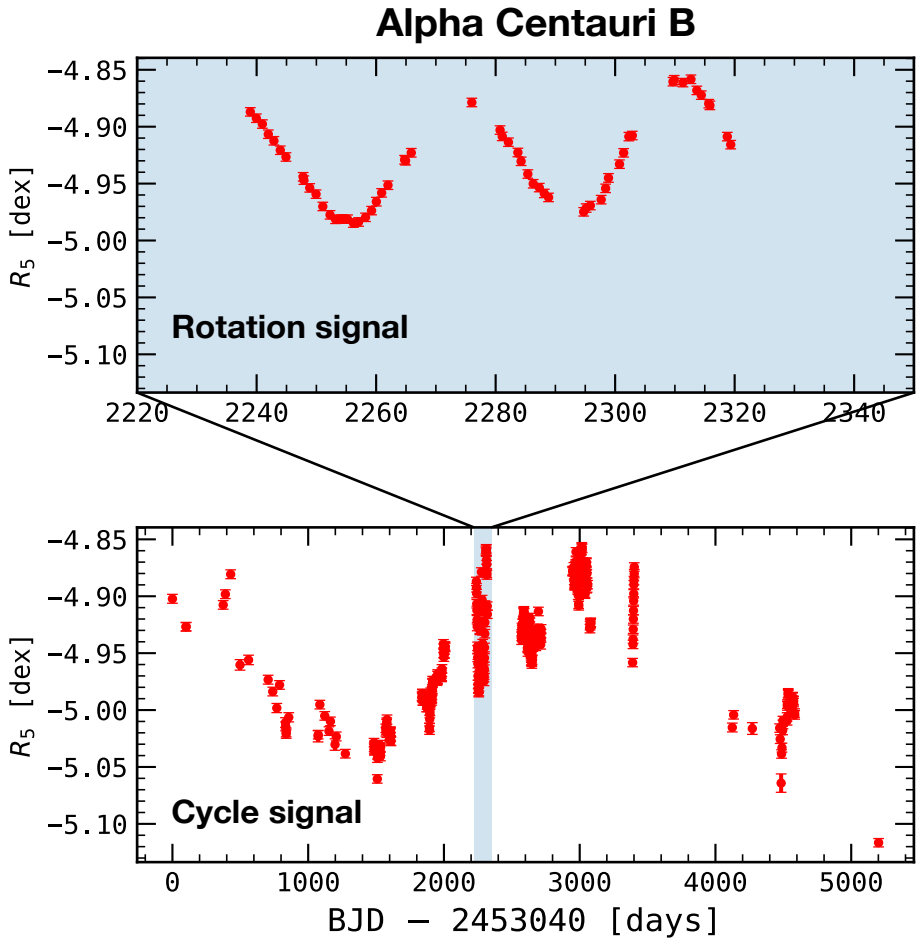

Aiming at a 20% age precision with gyrochronology and chromospheric activity

Possible, but only for a subset of PLATO targets

Main limitations and conclusions

- Gyrochronology has several limitations, especially for stars at the solar age or older because of the difficulty in determining the rotation period, the rather larger differential rotation, and the weakened braking phenomenon;

- Stars less massive than the Sun may suffer a prolonged phase of stalled rotational evolution (up to 1 Gyr for late-K or M-type stars);

- Therefore, *it seems safe to apply gyrochronology from F8 to G-type stars with ages in the range 0.7-4.5 Gyr*;

- We expect PLATO to help the calibration of gyrochronology for older stars and possibly for later-type stars, exploring metallicity effects (e.g., Amard et al. 2020);

- *The chromospheric-activity age (CA-A) relationship seems to hold up to 6-7 Gyr for solar twins*, but it requires an appropriate sampling of the intrinsic variations in the R'_{HK} index (rotation, active region evolution, and activity cycles) and to take into account metallicity effects;

- The physical reason for a weakened magnetic braking, while the CA-A relationship still holds at ages older than the Sun, is still unclear;

- It has been suggested that the stellar magnetic field may change its topology at the solar age, possible as a result of a change in the regime of differential rotation that affects the stellar dynamo (e.g., Metcalfe et al. 2021, 2022 and references therein; see theoretical models by Brun et al. 2017, 2022 and the recent work by Noraz et al. 2022);

Thank you very much for your attention

Additional material

R'_{HK} activity index determination

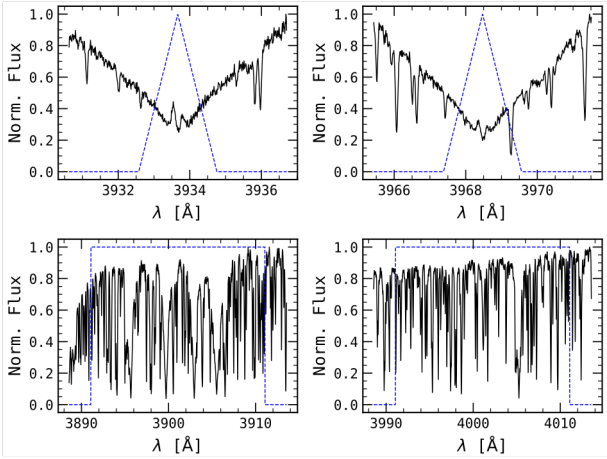

Fig. 6. Example of the bandpasses used to calculate $S_{\rm CaII}$ using a spectrum of τ Ceti. *Upper panels*: Ca II K line (*left*) and Ca II H line (*right*). *Lower panels*: Ca II blue reference band (*left*) and red band (*right*). Blue dashed lines are the bandpass functions.

$$S_{\rm CaII} = \frac{F_{\rm H} + F_{\rm K}}{R_{\rm B} + R_{\rm R}},$$

$$S_{\rm MW} = 1.195\,(\pm 0.035) \cdot S_{\rm CaII} + 0.008\,(\pm 0.007).$$

$$R'_{\rm HK} = R_{\rm HK} - R_{\rm phot},$$

$$R_{\rm HK} = 1.34 \times 10^{-4}\, C_{\rm cf}\, S_{\rm MW} \quad (5)$$

is the index corrected for bolometric flux (Middelkoop 1982), $C_{\rm cf}$ is the bolometric correction, and $R_{\rm phot}$ is the photospheric contribution. The photospheric contribution is a function of $B-V$ colour and has been discussed by Hartmann et al. (1984) and derived by Noyes et al. (1984) as

$$\log R_{\rm phot} = -4.898 + 1.918\,(B-V)^2 - 2.893\,(B-V)^3. \quad (6)$$

use the Rutten (1984) bolometric corrections:

$$\log C_{\rm cf} = 0.25(B-V)^3 - 1.33(B-V)^2 + 0.43(B-V) + 0.24$$

for main-sequence stars with $0.3 \le (B-V) \le 1.6$, and

$$\log C_{\rm cf} = -0.066(B-V)^3 - 0.25(B-V)^2 - 0.49(B-V) + 0.45 \quad (8)$$

for subgiant and giant stars with $0.3 \le (B-V) \le 1.7$.

(after Gomes da Silva et al. 2021)

The R'_{HK} index in field stars and in stars with transiting planets

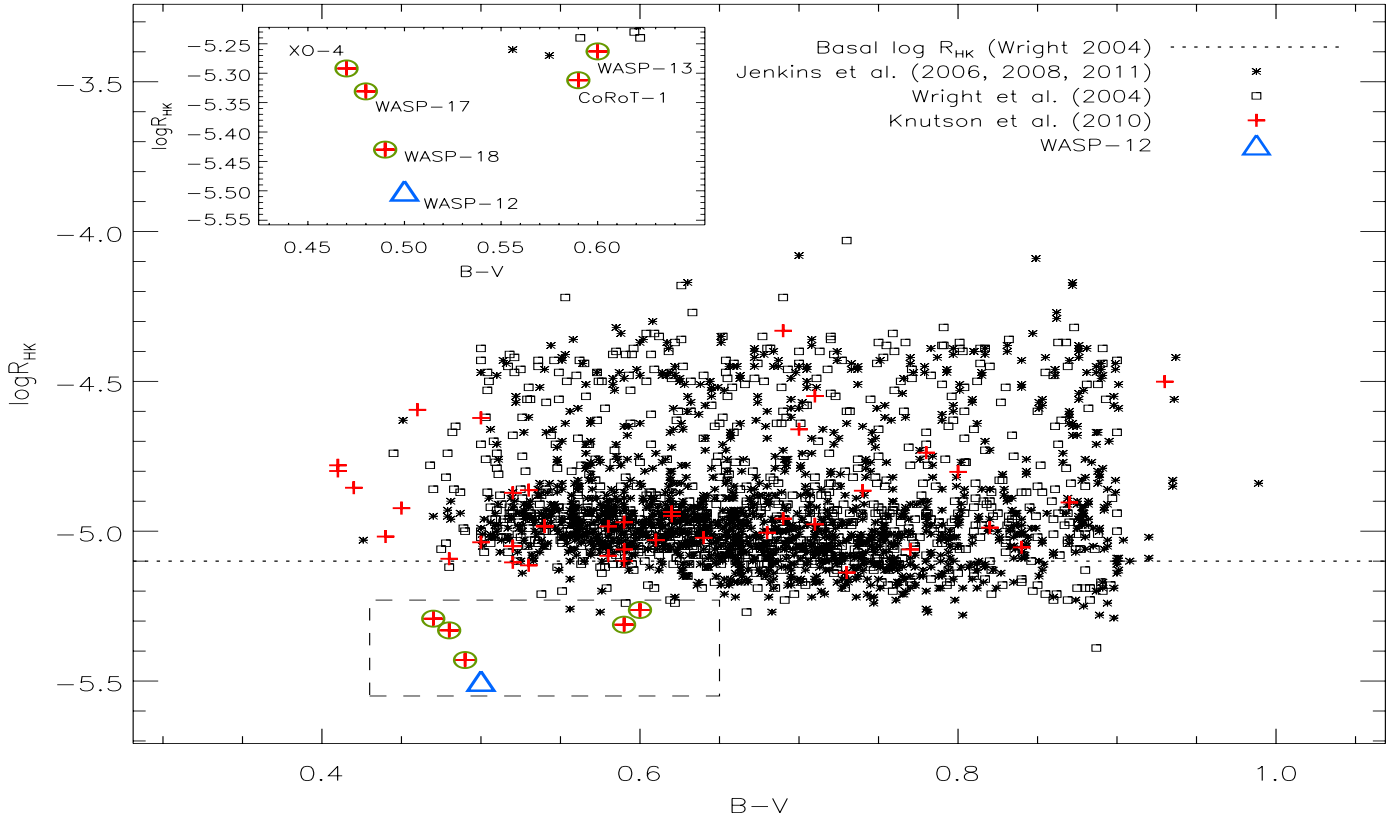

(after Fossati et al. 2013; see also statistical studies in Lanza 2014 and Fossati et al. 2015 interpreting the underactive stars as enshrouded by an absorbing plasma torus produced by planet evaporation or Pillitteri et al. 2014, Fossati et al. 2018 claiming a stellar dynamo quenching in WASP-18)

Metallicity effect on chromospheric index

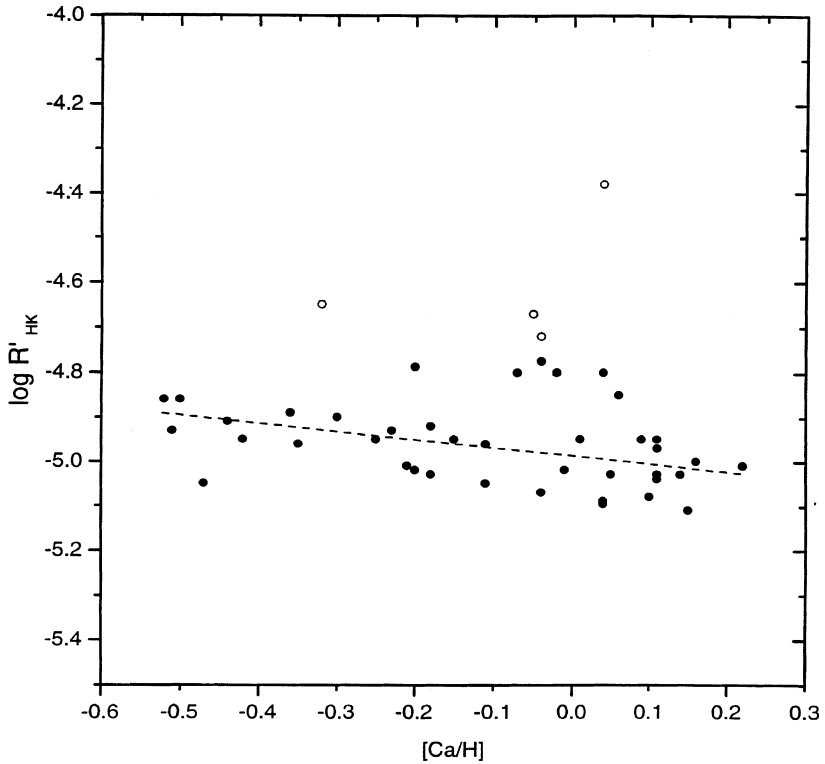

Figure 2. CE index as a function of the Ca abundances for the stars in Sample A. The values of [Ca/H] are from Edv93. Open circles: active stars; filled circles: inactive stars.

(Rocha-Pinto & Maciel 1998)

Metallicity effects on the activity-age relationship

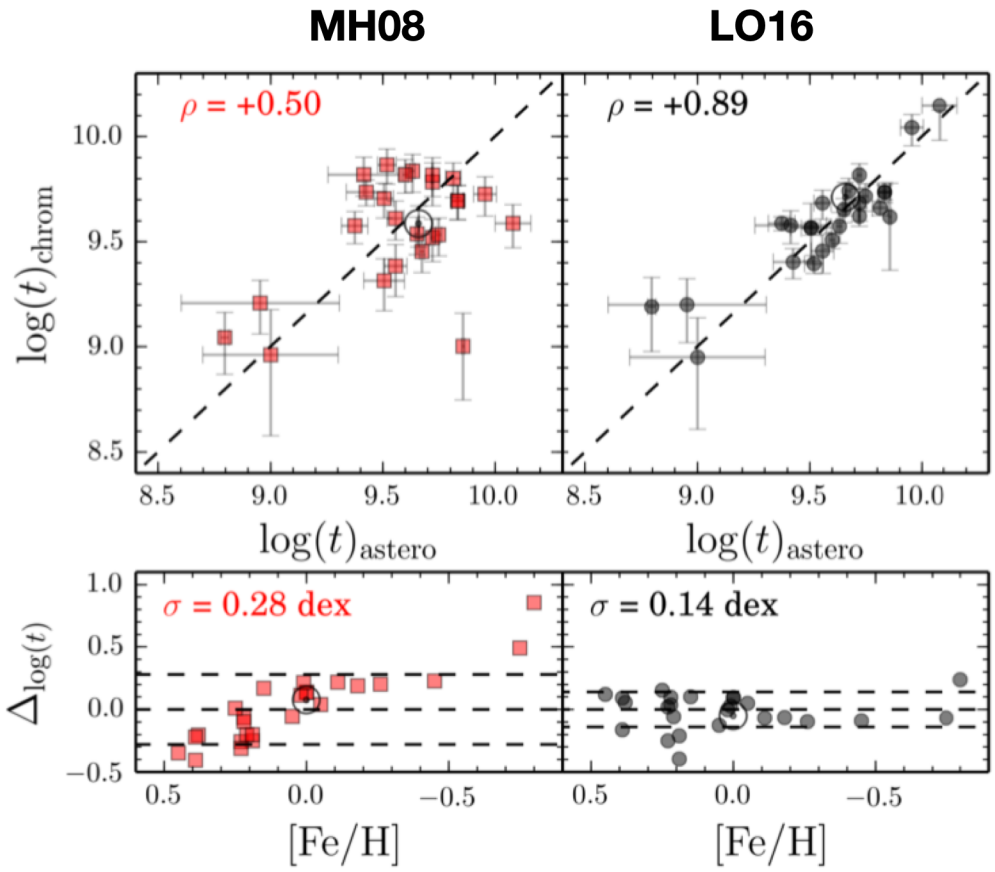

From the presentation of Joao Gomes da Silva at HOW#2.

Gallet & Bouvier (2015) AME model

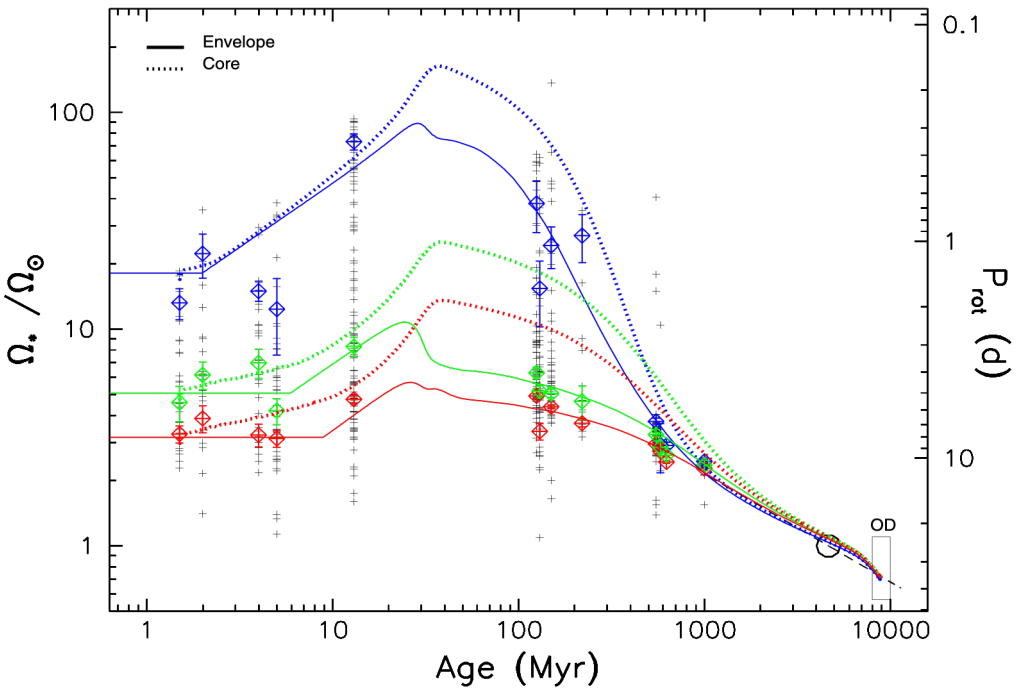

(a) 1 $M_\odot$

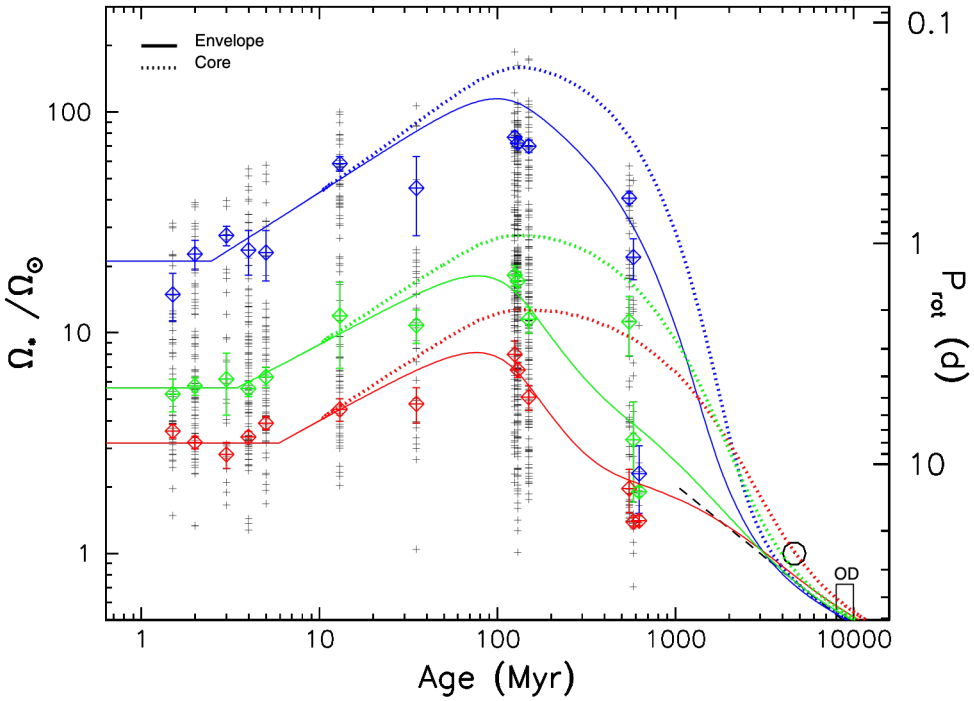

(c) 0.5 $M_\odot$

Chromospheric index vs. asteroseismic age

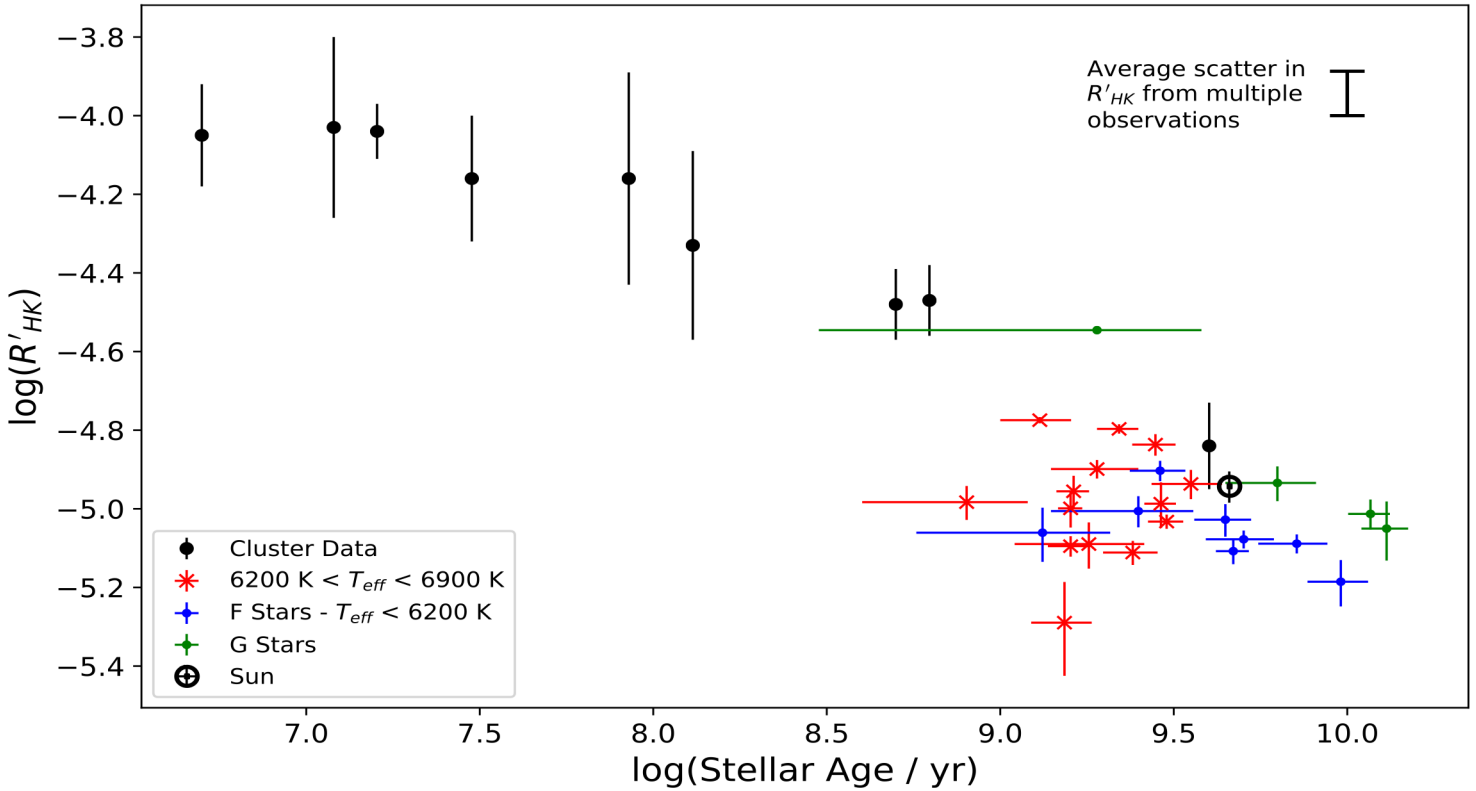

Figure 3. Plot showing data analysed in this work alongside cluster data from Mamajek & Hillenbrand (2008) shown in black. Early F-ype stars (with $T_{\rm eff}$ > 6200 K) are shown as red markers, later F-type stars (with $T_{\rm eff}$ < 6200 K) are denoted by blue markers and G-type stars are denoted by green markers. The average solar value over several cycles is also shown (Egeland et al. 2017).

(Booth et al. 2020, MNRAS 491, 455)

Possible evolution of the activity cycle periods

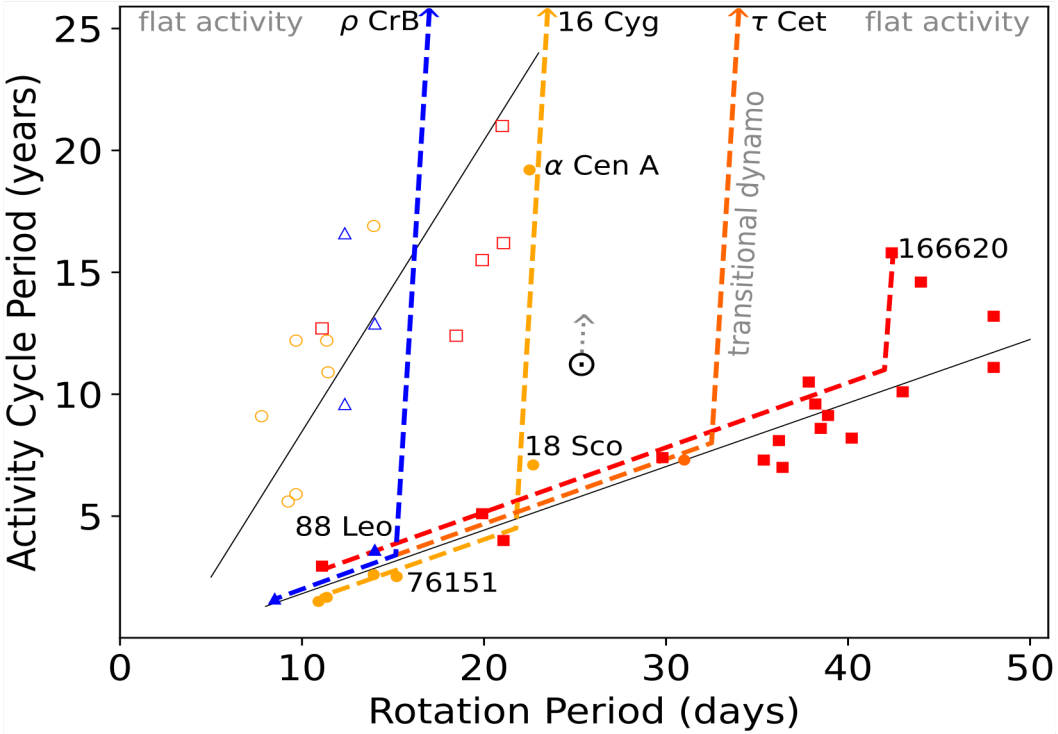

Figure 2. Dependence of activity cycle period on rotation, showing two distinct sequences (solid lines). Points are colored by effective temperature, indicating F-type (blue triangles), G-type (yellow and orange circles), and K-type stars (red squares). Schematic evolutionary tracks are shown as dashed lines (Metcalfe & van Saders 2017 and references therein), leading to stars with constant activity that appear to have shut down their global dynamos (arrows along the top).

(after Metcalfe et al. 2022, ApJ 933, L17)